Rotationally resolved photoelectron spectra from vibrational autoionization of NO Rydberg levels

Hongkun Park and Richard N. Zare
Department of Chemistry, Stanford University, Stanford, California 94305

(Received 3 September 1996; accepted 25 October 1996)

Rotationally resolved photoelectron spectra from vibrational autoionization of individual rotational levels of the nl_R ($v=1$, $11\leqslant n\leqslant 15$, $0\leqslant l_R\leqslant 3$) Rydberg states of NO are measured by combining two-color double-resonance excitation via the NO $A\ ^2\Sigma^+$ ($v_i=1$, $N_i=19$) state with time-of-flight photoelectron spectroscopy. The photoelectron spectra show that both even-l and odd-l continuum partial waves are generated by the autoionization events, and thus provide evidence for angular momentum exchange between the outgoing electron and the molecular-ion core. We interpret these observations as caused by the multipolar interactions between the outgoing electron and the vibrating nuclear core, which appear to be brought about both by the dependence on internuclear distance of the electron-ion-core electronic interaction and by Rydberg-valence state couplings. [S0021-9606(97)01905-3]

I. INTRODUCTION

In high-lying Rydberg states of a molecule, the semiclassical time scale associated with the Rydberg electronic motion is comparable to or even longer than those associated with the nuclear degrees of freedom.[1] Hence the Born–Oppenheimer approximation, which forms the basis for our understanding of low-lying electronic states of molecules, often breaks down in these states, and the coupling between the electronic and nuclear degrees of freedom plays an essential role in determining the dynamics of high-lying Rydberg states.[2,3] Vibrational autoionization of a molecule, in which the vibration of the nuclear framework drives an electron in a Rydberg state above the ionization limit to escape into the continuum, represents an especially dramatic example of the breakdown of the Born–Oppenheimer approximation.[3,4] Most experimental investigations of this phenomenon to date have been performed by various spectroscopic techniques, in which positions, widths, and intensities of Rydberg transitions have been measured.[5–8] Multichannel quantum defect theory (MQDT), which provides a unified theoretical framework for describing the dynamics of Rydberg states, has often been successfully applied to explain these spectroscopic observations.[3] Although the synergistic interplay between the various spectroscopic studies and MQDT has yielded valuable insight into the dynamics of vibrational autoionization, a quantitative understanding of this process has rarely been accomplished because of the experimental difficulties in probing the final quantum states associated with the various decay pathways.

High-resolution photoelectron spectroscopy coupled with multiple-resonance multiphoton excitation provides an ideal experimental probe for the dynamics of vibrational autoionization because it allows for the resolution of the quantum states of the ion and the photoelectron produced from vibrational autoionization of a well-defined quantum level in the high-lying Rydberg state. Most importantly, the resolution of the ion rotational states and the measurement of photoelectron angular distributions (PADs) associated with them enable the partial-wave decomposition of the ionization continuum, and provide a very detailed insight into the ionization dynamics of molecules.[9–17] Although many photoelectron spectroscopic studies have been performed to measure the vibrational state distributions of the ion[18,19] and to measure PADs associated with each vibrational state[20–22] following the vibrational autoionization events, the resolution of the rotational state of the ion has been achieved only for vibrational autoionization of H_2[23,24] and NO.[25]

The NO molecule has served as an important benchmark system for dynamical studies of high-lying Rydberg states of diatomic molecules.[22,26–43] The level-position analyses of high-lying Rydberg series of NO indicate that the electronic orbital angular momentum quantum numbers l_R of p and f Rydberg electrons are relatively unperturbed.[27,33] The $s\sigma$ and $d\sigma$ Rydberg series are, on the other hand, found to mix almost completely with each other to form so-called ''s,d supercomplexes.''[33,44] Despite the well-understood level structures of these Rydberg series, the detailed understanding of the decay dynamics of the nl_R Rydberg states has proven difficult because of the complexities that arise from interactions between the Rydberg levels and valence electronic states.[27,41–43,45–47] Direct measurements of the atomic nitrogen fragments from predissociation show that the nl_R Rydberg states ($0\leqslant l_R\leqslant 3$) of NO exhibit competition between vibrational autoionization and predissociation when both channels are open.[36,39,40] The measurements of line widths of individual Rydberg states suggest that this competition is strongly dependent on l_R;[29,35,38] whereas predissociation dominates the decay dynamics of the p Rydberg states, it does not play a major role in the $s\sigma$, $d\sigma$ Rydberg supercomplexes. Recently, several MQDT calculations have been performed to explain various experimental findings,[22,41–43] and they were partially successful in accounting for the observed widths of the np Rydberg levels[27,29] and the vibrationally resolved PADs from vibrational autoionization of the ns and nf Rydberg levels.[22] These calculations have explicitly con-

sidered the interactions between the Rydberg levels and various valence states but assumed that the orbital angular momentum of the Rydberg electron does not change during the autoionization process.[22,41–43]

In a previous report, we presented rotationally resolved photoelectron spectra from vibrational autoionization of the np and nf Rydberg levels of NO excited via the NO $A\ ^2\Sigma^+(v_i=1,\ N_i=19)$ state.[25] Those photoelectron spectra illustrate the production of many continuum partial waves with different electronic orbital angular momenta, $\vec{l}$, thus providing unequivocal experimental evidence for angular momentum exchange between the electronic and nuclear degrees of freedom in these autoionization events. In this article, we extend our previous study and report the rotationally resolved photoelectron spectra from vibrational autoionization of the nl_R $(11\leqslant n\leqslant 15,\ 0\leqslant l_R\leqslant 3)$ Rydberg levels of NO including the ns Rydberg levels. The spectra presented here indicate that the angular momentum exchange between the outgoing electron and the ion core is indeed a general characteristic of vibrational autoionization of high-lying Rydberg levels of NO. This observation is in sharp contrast with the observations made in vibrational autoionization of the singlet np Rydberg states of H_2,[24] for which the rotational state distributions of the H_2^+ ion were found to be consistent with the production of only p partial waves in the ionization continuum. The photoelectron spectra presented here also show that the rotational state distributions of the NO^+ ion are strongly dependent on various quantum numbers associated with the autoionizing Rydberg states. The partial-wave decomposition determined in our study clearly shows that the common assumption that the angular momentum for the Rydberg electron does not change in vibrational autoionization events is not generally valid.[8,22,41–43] Moreover, the detailed behavior of each Rydberg levels determined here provides an important insight into the dynamics of the vibrational autoionization of NO.

II. EXPERIMENT

A. Recording multiphoton ionization spectra

In the experiment reported here, the high-lying Rydberg levels of NO were prepared by two-color double-resonance excitation of NO via the NO $A\ ^2\Sigma^+$ $(v_i=1)$ state. In this excitation scheme, the first laser light (pump light) of wavelength λ_1 excites the NO molecule to a specific rotational level of the NO $A\ ^2\Sigma^+$ $(v_i=1)$ state, which is subsequently excited to various high-lying Rydberg levels by the second laser light (probe light) of wavelength λ_2. The two colors λ_1 and λ_2 were obtained from Nd:YAG-pumped pulsed dye lasers (DCR-3 and PDL-3, DCR-1A and PDL-1: Spectra Physics) operating at a repetition rate of 10 Hz. The pump color $(\lambda_1\approx 214$ nm) was generated by frequency doubling the dye laser output (PDL-3) using a β-barium borate (BBO) crystal. The probe color ($\lambda_2=311$–337 nm) was generated by frequency doubling the dye laser output (PDL-1) using a potassium dihydrogen phosphate (KDP) crystal.

The double-resonance multiphoton ionization (MPI) spectra were obtained in a stainless-steel gas cell filled with

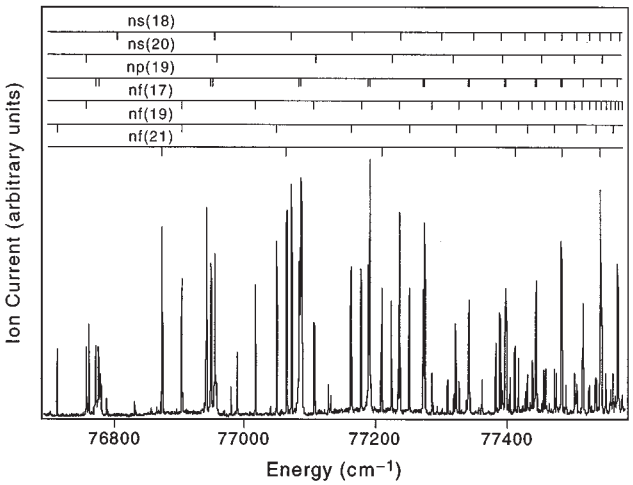

FIG. 1. A typical two-color double-resonance MPI spectrum of NO via the NO $A^2\Sigma^+$ $(v_i=1,\ J_i=18.5,\ N_i=19)$ level in a static gas cell. The NO pressure in the gas cell is 50 mTorr, and the voltage applied to the plates in the gas cell to collect ions is 10 V/cm. The level positions of $nl_R(N_R^+)$ Rydberg series of NO are indicated. The energy scale is referenced to the $X^2\Pi_{1/2}$ $(v=0,\ J=1/2)$ ground state of NO.

50 mTorr of neat NO.[25] Two counterpropagating laser beams were introduced into the gas cell through quartz windows, with the pump laser preceding the probe laser by ~10 ns. The NO^+ ions produced in the gas cell were collected with two metal plates by applying a static DC voltage on the order of 10 V/cm. Figure 1 shows a typical double resonance MPI spectrum via the NO $A\ ^2\Sigma^+$ $(v_i=1,\ J_i=18.5,\ N_i=19)$ level. An enlarged portion of this spectrum was presented in Fig. 1 of our previous publication.[25] The pump laser was tuned to 213.9 nm to be in resonance with the NO $A-X$ (1,0) $R_{21}(17.5)$ line, and the probe laser was scanned between the NO^+ $X^1\Sigma^+$ $(v^+=0)$ and the NO^+ $X^1\Sigma^+(v^+=1)$ ionization thresholds. Over 100 well-resolved resonance features are observed in the spectrum, each of which can be unambiguously assigned to the nl_R $(n\leqslant 40,\ 0\leqslant l_R\leqslant 3)$ Rydberg series of NO converging to the NO^+ $X\ ^1\Sigma^+$ $(v^+=1,\ N^+=17$–$21)$ ion (see Sec. III A). Level positions and widths of the spectral features did not change appreciably as a function of the collection voltage (<30 V/cm), indicating that the perturbations caused by the applied electric field are not significant for the Rydberg levels observed in the spectrum. Most of the background ion current in the spectrum is found to be caused by the one-color two-photon ionization of NO by the 213.9 nm pump light. Although it is not shown here, the double-resonance MPI spectrum via the NO $A\ ^2\Sigma^+(v_i=1,\ J_i=20.5,\ N_i=21)$ level was also obtained using the same experimental set up. The comparison of that spectrum with Fig. 1 facilitated the unambiguous assignment of spectral features because several main Rydberg series appeared in both spectra.

B. Recording photoelectron spectra

Once each spectral feature in the double-resonance MPI spectrum was assigned to a specific member of a Rydberg series, the probe laser was tuned to the peak position of a

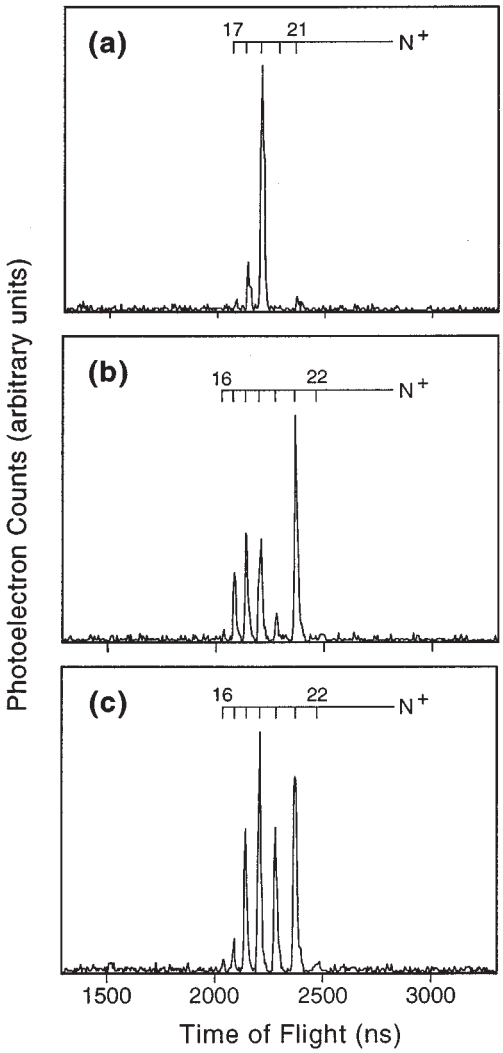

FIG. 2. Time-of-flight photoelectron spectra from vibrational autoionization of (a) the NO $13p$ ($v=1$, $N=19$, $N_R^+=19$) level, (b) the $13p$ ($v=1$, $N=18$, $N_R^+=19$) level, and (c) the $13p$ ($v=1$, $N=20$, $N_R^+=19$) level.

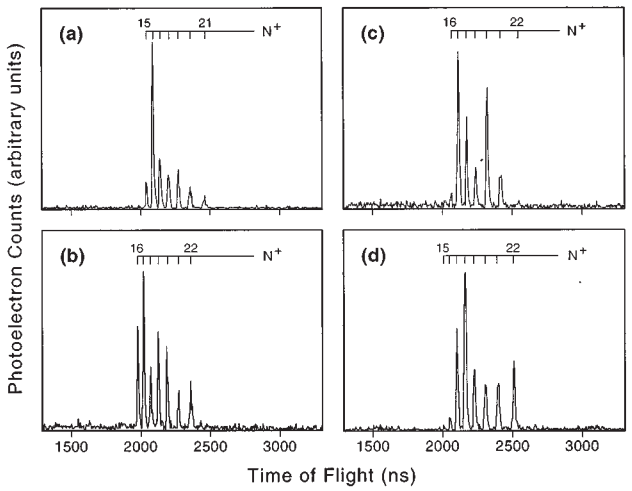

FIG. 3. Time-of-flight photoelectron spectra from vibrational autoionization of (a) the NO $13f$ ($v=1$, N, $N_R^+=17$) level, (b) the $15f$ ($v=1$, N, $N_R^+=17$) level, (c) the $12f$ ($v=1$, N, $N_R^+=19$) level, and (d) the $11p$ ($v=1$, N, $N_R^+=21$) level.

selected Rydberg level, and the photoelectron spectrum was recorded in a field-free time-of-flight (TOF) photoelectron spectrometer that has been described in detail previously.[10,48] All the photoelectron spectra reported here were obtained by setting the linear polarization vectors of both laser beams to point along the flight axis of the photoelectron spectrometer. Typically, the power of the pump laser was held below 1 μJ per pulse whereas that of the probe laser was approximately 100 μJ per pulse. Under these experimental conditions, the photoionization of NO by the absorption of two successive 213.9 nm photons was minimized, and only photoelectrons that resulted from the two-color two-photon absorption via the NO $A\ ^2\Sigma^+$ ($v_i=1$, $J_i=18.5$, $N_i=19$) level were recorded. The photoelectron counts approached the background level when the probe laser was tuned off resonance from a selected Rydberg feature, which indicates that the photoelectron peaks observed in our experiment result from the vibrational autoionization of the resonantly excited Rydberg level. The fact that the Rydberg features observed in the MPI spectrum in Fig. 1 show symmetric line profiles also suggests that we can ignore the direct photoionization of the NO $A\ ^2\Sigma^+$ ($v_i=1$) molecules to the ionization continuum associated with the $NO^+\ X\ ^1\Sigma^+$ ($v^+=0$) ion.[49] The magnetic field inside our spectrometer is measured to be less than 5 mG,[11] and the electric field inside the spectrometer is estimated to be on the order of 1 mV/cm based on the photoelectron flight time and the photoelectron energy resolution ($\leqslant$2 meV).

Figures 2–5 present typical photoelectron spectra that result from vibrational autoionization of high-lying Rydberg levels of NO. Fully resolved photoelectron peaks that correspond to production of ions in different rotational levels of $NO^+\ X\ ^1\Sigma^+$ ($v^+=0$) are clearly discernible. Each photoelectron peak is denoted by the rotational quantum number N^+ of the $NO^+\ X\ ^1\Sigma^+$ ($v^+=0$) ion. The assignment of each photoelectron peak in the spectra was achieved through a careful energy calibration of our photoelectron spectrometer using the photoelectrons from the direct photoionization of NO $A\ ^2\Sigma^+$ ($v_i=1$, $J_i=18.5$, $N_i=19$) above the $NO^+\ X\ ^1\Sigma^+$ ($v^+=1$) ionization threshold. Because the rotational state distribution from this direct photoionization event is known[11] and also because the photoelectron energy can be precisely controlled by varying the wavelength of the ionizing laser light, the value of N^+ associated with each photoelectron peak in Figs. 2–5 could be determined unambiguously by comparing these spectra with those obtained from the direct photoionization of NO.

III. RESULTS AND DISCUSSION

A. Structure of the autoionizing Rydberg levels

The NO $A\ ^2\Sigma^+ - X\ ^2\Pi$ transition is well understood and needs no further discussion.[26] The transitions from the NO $A\ ^2\Sigma^+$ ($v_i=1$) state to the high-lying Rydberg states of NO converging to the $NO^+\ X\ ^1\Sigma^+$ ($v^+=1$) ion have also been studied extensively using double-resonance MPI and fluores-

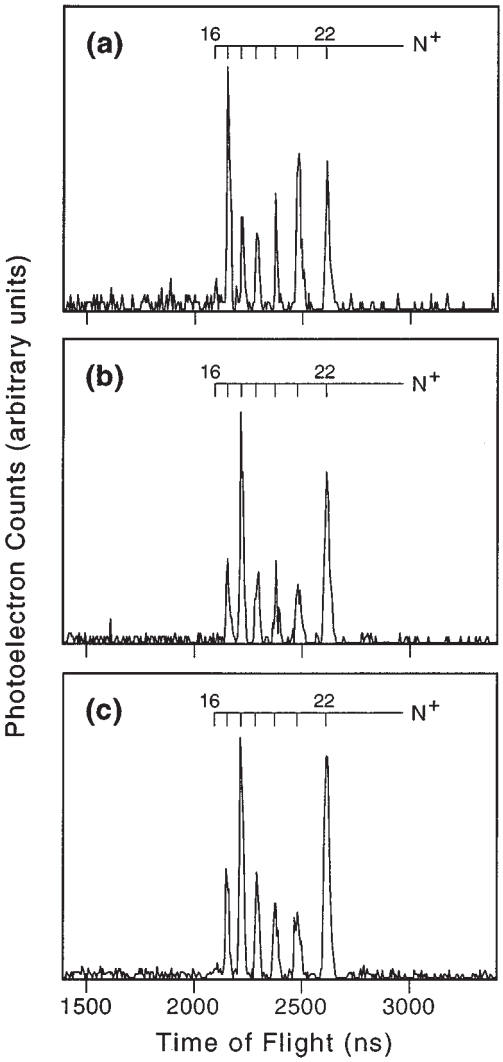

FIG. 4. Time-of-flight photoelectron spectra from vibrational autoionization of (a) the NO $12f$ ($v=1$, $N=18$, $N_R^+=21$) level, (b) the $12f$ ($v=1$, $N=19$, $N_R^+=21$) level, and (c) the $12f$ ($v=1$, $N=20$, $N_R^+=21$) level.

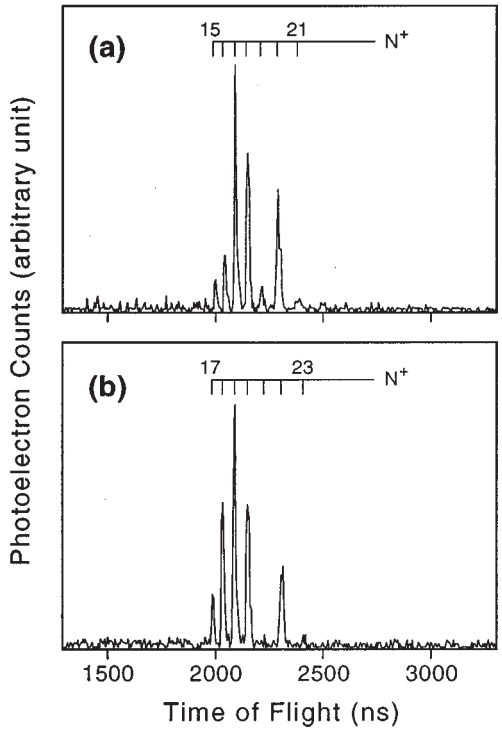

FIG. 5. Time-of-flight photoelectron spectra from vibrational autoionization of (a) the NO $14s$ ($v=1$, $N=18$, $N_R^+=18$) level, and (b) the $14s$ ($v=1$, $N=20$, $N_R^+=20$) level.

cence dip spectroscopy.[29,30,32,34,35,37,38] The main difference between the present study and those reported earlier is that the Rydberg levels observed in this study are associated with high rotational quantum numbers ($N \geqslant 18$) whereas the previous studies concentrated on Rydberg levels with $N \leqslant 10$. Although the basic physics that determines the rotational level structure of these high-N Rydberg levels remains the same as that for the low-N Rydberg levels,[20,30,34] some discussion of the double-resonance MPI spectrum in Fig. 1 is still warranted because the detailed understanding of it is important in the subsequent analyses of photoelectron spectra. As is well known,[2] the electronic character of each Rydberg level changes as a function of the rotational quantum number because of heterogeneous interactions between Rydberg levels, knowledge of which provides a vital insight into the dynamics of each Rydberg level.

The Rydberg levels of NO with principal quantum numbers greater than 10 follow closely Hund's case (d) coupling,[29,30,32,34,35,37,38] and thus can be designated by angular momentum quantum numbers N and N_R^+.[2,50,51] Here $\vec{N}$ represents the total angular momentum excluding electronic and nuclear spin, and $\vec{N}_R^+$ represents the nuclear rotation plus electronic orbital angular momentum for the NO^+ ion core. The distinction between the quantum numbers N_R^+ and N^+ should be clearly noted: whereas N_R^+ denotes the rotational quantum number of the ion core in the Rydberg state, N^+ denotes the rotational quantum number of the bare ion. The NO $A\ ^2\Sigma^+$ ($v_i=1$) state, on the other hand, follows Hund's case (b) coupling. The angular momentum quantum numbers that designate this state are N and Λ, where Λ represents the projection of electronic orbital angular momentum $\vec{l}_R$ on the molecular axis. The electric dipole selection rule for one-photon absorption dictates that only transitions with $\Delta N = 0, \pm 1$ and that involve parity change are possible for the transition between states that belong to Hund's case (b) and (d) coupling cases.[52]

Upon close inspection of the double-resonance MPI spectrum in Fig. 1, seven Rydberg series converging to the $NO^+\ X\ ^1\Sigma^+$ ($v^+=1$, N^+) ion are clearly discernible. In addition, more than a dozen peaks that do not belong to these main Rydberg series are also observed in the spectrum. Each of the main Rydberg series was analyzed by fitting the level positions of its members to the well-known Rydberg formula,

$$T_n(v, l_R, N) = T_\infty(v^+=1, N^+) - \frac{\mathrm{Ryd_{NO}}}{(n-\mu_{v,l_R,N})^2}. \qquad (1)$$

TABLE I. Quantum defects and the series limits for the observed Rydberg series. The quantum defects given in the third column are those reported for the low N levels (Ref. 32). The theoretical series limits presented in the last column are calculated from the spectroscopic constants of NO^+ (Ref. 26).

Rydberg series	$\mu_{v,l_R,N}$		$T_\infty(v^+=1,N^+=N_R^+)\,(\mathrm{cm}^{-1})$	
nl_R $(v=1, N, N_R^+)$	This study	low N	This study	Calculated
ns $(v=1, 18, 18)$	1.175(7)	1.178	77738.5(5)	77738.8
ns $(v=1, 20, 20)$	1.180(8)	1.118	77893.2(9)	77892.3
np $(v=1, 19, 19)$	0.7448(9)	0.729	77813.5(9)	77813.6
np $(v=1, N, 19)$	0.720(3)	0.722	77813.4(3)	77813.6
nf $(v=1, N, 17)$	0.027(3)	0.033	77667.7(2)	77667.9
nf $(v=1, N, 19)$	0.021(1)	0.021	77813.4(1)	77813.6
nf $(v=1, N, 21)$	0.026(3)	0.025	77974.9(4)	77975.0

In Eq. (1), $\mathrm{Ryd_{NO}}$ represents the Rydberg constant of NO corrected for the mass of NO ($\mathrm{Ryd_{NO}}=109735.306\ \mathrm{cm}^{-1}$), $T_n(v,l_R,N)$ represents the energy of the n-th member of the (l_R,N) Rydberg series converging to the NO^+ $X\ ^1\Sigma^+(v^+=1,\ N^+)$ ion, T_∞ $(v^+=1,\ N^+)$ represents the corresponding series limit, and $\mu_{v,l_R,N}$ represents the quantum defect for the corresponding Rydberg series. In our fit, the dependence of $\mu_{v,l_R,N}$ on the principal quantum number n is ignored because this dependence is expected to be negligible in the spectral range measured in our experiment. The effect of vibrational autoionization on the Rydberg level positions was also ignored in our fit.[30,32,33]

The results of fitting the seven Rydberg series that appear in the spectrum to Eq. (1) are given in Table I. Based on the well-known spectroscopic constants of the NO^+ $X\ ^1\Sigma^+$ ion[53] and the quantum defects for low-n Rydberg levels,[26] it is straightforward to assign the observed series to a specific nl_R $(v=1,\ N,\ N_R^+)$ Rydberg series. The assignments are listed in the first column of Table I. They are also included in Fig. 1 as horizontal bars. As shown in Table I, the quantum defect parameters obtained in our fit agree very well with those obtained in the previous studies for the Rydberg states with lower rotational quantum numbers.[29,30,32,34,35] The double-resonance MPI spectrum in Fig. 1 shows that the N substructures of the np Rydberg levels were only partially resolved. The fine structures of the nf Rydberg states were, on the other hand, unresolved within the bandwidth of our laser. The spectrum illustrates that the linewidths for the np Rydberg levels are significantly broader ($\approx 1.5\ \mathrm{cm}^{-1}$) than those for the ns and nf Rydberg levels. This line broadening is consistent with the previous observations of the np Rydberg states with lower N,[29,32,34,39,41,42,54] and stems from the fast predissociation of the np Rydberg levels.[41,42] Because of the broad bandwidth ($\approx 0.5\ \mathrm{cm}^{-1}$) of the probe laser employed in this work, the detailed analysis of the line widths for individual Rydberg levels was not performed.

Although the Hund's case (d) description of the Rydberg levels is appropriate for the level position analysis, it does not provide a deep insight into the interaction between the Rydberg electron and the ion core because the interactions responsible for vibrational autoionization occur near the ion core where the Hund's case (b) designation is more appropriate.[3,16] In principle, the wave function expressed in the Hund's case (d) coupling scheme can be expanded in terms of the Hund's case (b) wave functions by a simple geometric frame transformation.[55,56] However, as evidenced by the splitting of various N sublevels, the Rydberg levels of NO observed in the present experiment do not follow Hund's case (d) coupling exactly. For this reason, the wave function for each Rydberg level was obtained by diagonalizing the molecule-fixed-frame rotational Hamiltonian using the Hund's case (b) basis functions.[30,57] The vibronic term energies necessary for the calculation were adapted from Ref. 30. The molecular Hamiltonian includes the l-uncoupling operator responsible for the heterogeneous perturbations between the Rydberg series. The spin part of the Hamiltonian was omitted in our calculation, however, because spin-orbit and spin-rotation couplings are known to be small in the high-lying Rydberg states of NO.[26]

It is well established from the MQDT analysis of the Rydberg level structures that the electronic orbital angular momentum quantum numbers l_R of the p and f Rydberg electrons are relatively unperturbed.[26,33] Therefore, for the np and nf Rydberg series, the l-uncoupling operator couples only the levels within the same l manifolds, and the diagonalization of the rotational Hamiltonian is relatively straightforward. On the other hand, the mixing between the $s\sigma$ and $d\sigma$ Rydberg series is known to be almost complete.[27,33,44] Because of this homogeneous l-mixing interaction, the ''s'' Rydberg levels observed in Fig. 1 possess $s\sigma$, $d\sigma$, $d\pi$, and even $d\delta$ character. In our calculation, the strength of the $s\sigma-d\sigma$ interaction was assumed to be the same as that determined by Fredin *et al.*[33] for high-lying Rydberg levels converging to the NO^+ $X\ ^1\Sigma^+(v^+=0)$ ion. The effect of the l-uncoupling operator on the d Rydberg manifold was treated explicitly.

The results of the calculation for selected Rydberg levels are collected in Table II. In addition to enabling the characterization of the observed Rydberg levels in terms of the Hund's case (b) basis functions, the calculation also allows us to predict the positions of the individual N sublevels for the p and f Rydberg series that are unresolved. In general, the level positions obtained in this calculation are found to reproduce the experimental level positions with an accuracy better than $1\ \mathrm{cm}^{-1}$. Considering the experimental uncertainties associated with our laser bandwidth and the calibration

TABLE II. The electronic character of selected Rydberg levels near the molecular-ion core.

Rydberg levels	Electronic character (in %)									
nl_R $(v=1,\ N,\ N_R^+)$	$s\sigma$	$p\sigma$	$p\pi$	$d\sigma$	$d\pi$	$d\delta$	$f\sigma$	$f\pi$	$f\delta$	$f\phi$
13p (1, 18, 19)	⋯	54	46	⋯	⋯	⋯	⋯	⋯	⋯	⋯
13p (1, 19, 19)	⋯	0	100	⋯	⋯	⋯	⋯	⋯	⋯	⋯
13p (1, 20, 19)	⋯	46	54	⋯	⋯	⋯	⋯	⋯	⋯	⋯
12f (1, 18, 21)	⋯	⋯	⋯	⋯	⋯	⋯	34	48	16	2
12f (1, 19, 21)	⋯	⋯	⋯	⋯	⋯	⋯	0	36	50	14
12f (1, 20, 21)	⋯	⋯	⋯	⋯	⋯	⋯	19	2	38	41
14s (1, 18, 18)	67	⋯	⋯	8	0	25	⋯	⋯	⋯	⋯
14s (1, 20, 20)	79	⋯	⋯	5	0	16	⋯	⋯	⋯	⋯

of the dye laser wavelength, the agreement between the calculated and observed level positions is deemed acceptable.

B. Rotationally resolved photoelectron spectra

Figures 2–5 show rotationally resolved photoelectron spectra from vibrational autoionization of various nl_R $(v=1, N, N_R^+)$ Rydberg levels of NO. All the spectra show clearly that many rotational levels of the NO^+ $X\ ^1\Sigma^+$ $(v^+=0)$ ion are populated after vibrational autoionization of the nl_R $(v=1)$ Rydberg levels with a given rotational quantum number N_R^+. Except for the photoelectron spectrum from vibrational autoionization of the 13p $(v=1, N=19, N_R^+=19)$ Rydberg level, all the spectra show several photoelectron peaks with comparable intensities. Inspection of Figs. 2–5 also reveals that the distributions of the ion rotational states depend strongly on the quantum numbers N_R^+ and N. The photoelectron spectra presented here, combined with the similar spectra reported previously,[25] show that the observed trends are not restricted to a few Rydberg levels but are a general characteristic of vibrational autoionization of nl_R Rydberg levels with $11 \leqslant n \leqslant 15$ and $0 \leqslant l_R \leqslant 3$.

The observed rotational state distributions of NO^+ provide information on the partial-wave decomposition of the continuum photoelectrons produced from vibrational autoionization of a given Rydberg level.[23–25] In our experiment, high-lying Rydberg levels of NO are excited from the NO $A\ ^2\Sigma^+$ $(v_i=1, N_i=19)$ level by one-photon dipolar absorption and then decays under the field-free condition into the NO^+ $X\ ^1\Sigma^+$ $(v^+=0, N^+)$ ion and a free electron. A simple parity consideration applied to this $\Sigma-\Sigma$ photoionizing transition yields the photoionization selection rule, $N^+-N_i+l=$odd.[58,59] This selection rule implies that the observation of even-N^+ peaks in our photoelectron spectra corresponds to the generation of even-l partial waves in the ionization continuum whereas the observation of odd-N^+ peaks corresponds to the generation of odd-l partial waves. In addition, information on the range of l generated in the ionization continuum can be obtained from the range of N^+ observed in our photoelectron spectra; because the total angular momentum is conserved in the vibrational autoionization process, three angular momentum vectors $\vec{N}$, $\vec{N}^+$, and $\vec{l}$ should meet the triangle condition in order for each l partial wave to be responsible for the N^+ photoelectron peaks in our spectrum.[60,61] Although the N substructures of the high-lying Rydberg levels are not always resolved in our experiment, N should range from 18 to 20 because N_i is 19.

The analysis of Figs. 2–5 based on these symmetry constraints reveal that many partial waves with different l values are produced in general by vibrational autoionization of nl_R Rydberg levels converging to the NO^+ $X\ ^1\Sigma^+$ $(v^+=1, N^+)$ ion. Specifically, Fig. 2(a) shows that mostly p waves are produced by vibrational autoionization of the 13p $(v=1, N=19, N_R^+=19)$ level although a small amount of even-l partial waves are also produced in the ionization continuum as evidenced by the small $N^+=18$ peak. Figures 2(b) and 2(c) show, on the other hand, that the behavior of the 13p $v=1$, $N=18$ and 20, $N_R^+=19$) levels is rather different from that of the 13p $(v=1, N=19, N_R^+=19)$ level. Figures 2(b) and 2(c) are obtained by fixing the probe laser wavelengths at the predicted positions of the 13p $(v=1, N=18, N_R^+=19)$ and 13p $(v=1, N=20, N_R^+=19)$ levels, respectively (see Sec. III A). Because the 13p $(v=1, N=18, N_R^+=19)$ and 13p $(v=1, N=20, N_R^+=19)$ levels are not well resolved in our experiment, the spectra in Figs. 2(b) and 2(c) should have contributions from both of these quantum levels. The relative contribution of the 13p $(v=1, N=18, N_R^+=19)$ and 13p $(v=1, N=20, N_R^+=19)$ levels should change, however, as a function of the probe laser wavelength, and the designations given for Figs. 2(b) and 2(c) represent the major contributors between these two levels. Both spectra indicate that p and possibly f partial waves dominate the ionization continuum when the 13p $(v=1, N=18$ and 20, $N_R^+=19)$ levels autoionize. The strong presence of even-N^+ peaks in these spectra indicates, however, that the contributions of even-l partial waves are more significant in these cases compared with vibrational autoionization of the 13p $(v=1, N=19, N_R^+=19)$ level.

Figures 3 and 4 show that vibrational autoionization of the nf $(v=1, N, N_R^+)$ levels populates more rotational levels of NO^+ than those of the np Rydberg levels. In vibrational autoionization of all the nf Rydberg levels, more than five photoelectron peaks with comparable intensities appeared in the spectra, which indicates that comparable amounts of even-l and odd-l partial waves are produced in the ionization continuum. Surprisingly, Figs. 3(a), 3(d), and 4(b) show that the strongest photoelectron peaks are associated with even-N^+ rotational states of the ion, which indicates that the ionization continuum may be dominated by even-l partial

waves despite the fact that the orbital angular momentum of the autoionizing electron itself is odd ($l_R=3$). It should be remembered, however, that the photoelectron spectra presented here do not provide sufficient information to determine the exact partial-wave decomposition of the ionization continuum because all the photoelectron spectra were recorded at a fixed laser-polarization geometry and also because the N substructures within the nf Rydberg features are not well resolved. In general, the intensity distributions in a photoelectron spectrum obtained at a fixed laser-polarization geometry does not represent the rotational branching ratio of a photoionization event because PADs associated with each rotational peak can be quite different from one another. Indeed, our preliminary study shows that the shapes of PADs depend strongly on the rotational quantum number N^+ of the ion for some vibrational autoionization events.[61]

The comparison of various photoelectron spectra in Fig. 3 demonstrates that the rotational state distributions of the NO^+ $X\ ^1\Sigma^+$ ($v^+=0, N^+$) ion vary significantly as a function of the principle quantum number n and the rotational quantum number N_R^+. Figure 4 illustrates, on the other hand, that the ion rotational distributions are also dependent on the quantum number N. Whereas the photoelectron spectra in Fig. 3 were obtained by fixing the probe laser wavelength at the peak positions of the corresponding Rydberg features, the spectra in Fig. 4 were obtained at three different probe laser wavelengths within the $12f$ ($v=1$, N, $N_R^+=21$) resonance profile, each separated by 0.6 cm^{-1}. The assignment of each spectrum to the individual N substructure was made based on the calculated positions of the $12f$ ($v=1$, N, $N_R^+=21$) levels. As was the case for the photoelectron spectra from vibrational autoionization of the $13p$ ($v=1$, $N=18$ and 20, $N_R^+=19$) levels, these assignments should be interpreted as denoting the major contributor to each photoelectron spectrum. Figure 4 nevertheless illustrates that the rotational state distribution of the ion depends on the quantum number N, although the dependence is not so strong as those on quantum numbers n and N_R^+ illustrated in Fig. 3. This reduced dependence may be intrinsic to the dynamics of the vibrational autoionization itself, or it may originate from our inability to excite the individual $12f$ ($v=1$, N, $N_R^+=21$) levels.

Figures 5(a) and 5(b) show the photoelectron spectra obtained from vibrational autoionization of the $14s$ ($v=1$, $N=18$, $N_R^+=18$) and the $14s$ ($v=1$, $N=20$, $N_R^+=20$) levels. The peak intensities in the photoelectron spectra did not change appreciably as the probe laser wavelength was scanned within each resonance profile. This observation confirms that the observed photoelectron spectra result from vibrational autoionization of individual Rydberg levels. As was the case for the vibrational autoionization events of the nf Rydberg levels, Figs. 5(a) and 5(b) show several photoelectron peaks with comparable intensities and indicate that significant amounts of odd-l partial waves are generated by vibrational autoionization of these even-l_R Rydberg levels. The most striking features in Figs. 5(a) and 5(b) are the intensities of the photoelectron peaks that correspond to the production of the NO^+ $X\ ^1\Sigma^+$ ($v^+=0$, $N^+=N+1$) ion. They are very weak in both spectra, whereas the photoelectron peaks for the NO^+ $X\ ^1\Sigma^+$ ($v^+=0$, $N^+=N-1$) ion are strong. According to the photoionization selection rule mentioned above, both $N^+=N-1$ and $N^+=N+1$ peaks result from the production of odd-l partial waves in the ionization continuum. Therefore the near absence of $N^+=N+1$ photoelectron peaks in Figs. 5(a) and 5(b) cannot be attributed to the absence of odd-l partial waves but instead should be attributed to interference between various odd-l partial waves in the ionization continuum.[15,17] The analysis of rotationally resolved PADs from the vibrational autoionization events indeed confirms this interpretation and will be discussed in a subsequent publication.[61]

C. Vibrational autoionization dynamics of NO

The analysis of the photoelectron spectra in Figs. 2–5 establishes unambiguously that many different continuum partial waves are generated from vibrational autoionization of rovibrationally state-selected ns, np, and nf Rydberg levels of NO. In general, photoelectron peaks associated with even-N^+ and odd-N^+ ion rotational states are observed in the photoelectron spectra, indicating that both even-l and odd-l partial waves are present in the ionization continuum irrespective of the electronic character of the autoionizing Rydberg state. As such, the photoelectron spectra in Figs. 2–5 present unequivocal experimental evidence for angular momentum exchange between the outgoing electron and the NO^+ core in vibrational autoionization of the nl_R ($11\leqslant n\leqslant 15$, $0\leqslant l_R\leqslant 3$) Rydberg levels of NO.

These observations are rather surprising considering that l_R values for both p and f Rydberg electrons are relatively unperturbed.[27,33] Although the $s\sigma$ and $d\sigma$ Rydberg series are found to mix almost completely with each other,[33,34] the analysis of the Rydberg-level positions indicates that mixing between the odd-l_R and even-l_R Rydberg series is not significant. As described in Sec. III A, the Rydberg level positions observed in Fig. 1 can be reproduced very well by a MQDT analysis that assumes only $s\sigma-d\sigma$ mixing. The photoelectron spectra in Figs. 2–5 show, on the other hand, that significant mixing occurs between even-l and odd-l partial waves induced by the vibrational quantum change of the NO^+ core. In the framework of MQDT, the dynamics of vibrational autoionization is governed by the derivatives of the molecule-frame reaction matrix elements, $K_{ll'}(R)$, with respect to the internuclear distance R, whereas the level structures of Rydberg states are roughly governed by the vibrationally averaged reaction matrix elements.[3,62,63] Therefore our experimental results indicate that $dK_{ll'}(R)/dR(l\neq l')$ can be of sizable magnitude even when the vibrationally averaged off-diagonal reaction matrix elements themselves are nearly zero. In previous theoretical calculations applied to vibrational autoionization, it has been commonly assumed that only $l=l_R$ partial waves are generated in the ionization continuum when the nl_R Rydberg states autoionize.[3,8,41–43,64,65] This assumption is equivalent to ignoring all the multipolar interactions between the Rydberg electron and the ion core except the monopolar interaction. The mixing between even-l and odd-l partial waves found in

our experiments suggests, on the other hand, that the interaction between the outgoing electron and the vibrating dipolar ion core plays an important role in vibrational autoionization of the ns and nf Rydberg states of NO.

Two types of interactions have been proposed to explain vibrational autoionization of molecules:[66] one is termed the ''vibrational'' or ''direct'' coupling mechanism, and the other is termed the ''electronic'' or ''indirect'' coupling mechanism. In the vibrational coupling mechanism, the coupling between the Rydberg levels and the nearby ionization continuum is caused by the dependence of the electron-ion-core interaction on the internuclear distance R. The electronic coupling, on the other hand, refers to the indirect coupling between the Rydberg state and the ionization continuum mediated by the strong electronic interactions between the Rydberg and valence states responsible for predissociation. The distinction between these two types of mechanisms originates from the particular choice of the Rydberg basis functions (or channel functions) in MQDT.[66] The Rydberg basis functions commonly employed in MQDT belong to the diabatic representation of the electronic states and do not diagonalize either the electronic or the nuclear kinetic-energy parts of the full molecular Hamiltonian.[2,66] The vibrational coupling mechanism refers to the Rydberg-continuum coupling caused by the off-diagonal matrix elements of the nuclear kinetic-energy part of the Hamiltonian, whereas the electronic coupling mechanism refers to the coupling caused by the off-diagonal matrix elements of the electronic part of the Hamiltonian.

In principle, the angular momentum exchange between the outgoing electron and the molecular ion core can be explained by either mechanism. In the vibrational coupling mechanism, the angular momentum exchange can be caused by the R dependence of the multipolar interaction between the Rydberg electron and the vibrating ion core.[67,68] In the electronic coupling mechanism, on the other hand, the partial-wave decomposition of the continuum electron should depend on the nature of the valence electronic state that is responsible for the indirect coupling. Unfortunately, however, it is impossible to determine which mechanism is more important in the vibrational autoionization events of NO based solely on the photoelectron spectra because both the vibrational and electronic coupling mechanisms are homogeneous perturbations in character.

As mentioned previously, many Rydberg-valence interactions have been identified based on spectroscopic deperturbation analyses[27,31,33,37] and measurements of the atomic nitrogen product from predissociation of various Rydberg states.[36,39,40] Many *ab initio* and MQDT calculations have also been performed to explain these experimental findings.[41–43,45–47] Among the Rydberg-valence interactions, the coupling between the $p\pi$ Rydberg series and the $B\ ^2\Pi$ and $L\ ^2\Pi$ valence states is known to be strongest.[27,41,42,45] The $p\sigma$ Rydberg series is, on the other hand, known to interact with the $A'^2\Sigma^+$ state.[27,46,47] In Fig. 1, these strong interactions are manifested as the line broadening of the p Rydberg features. Although they are not so strong as the interactions of the p Rydberg series, the interactions between the $f\sigma$ Rydberg series and the $A'^2\Sigma^+$ and $I\ ^2\Sigma^+$ states are also found to be significant.[39,40] Other proposed interactions include those between the $s\sigma$ and $d\sigma$ Rydberg series and the $I\ ^2\Sigma^+$ state and between the $d\delta$ series with the $B'^2\Delta$ state.[36,39,43,46,47]

Although it is impossible to assess the relative importance of the vibrational and the electronic coupling mechanisms based on our experiment alone, a comparison of our experimental findings with information on various Rydberg-valence interactions illustrates that both mechanisms need to be invoked to explain the partial-wave decomposition from vibrational autoionization of NO Rydberg levels. The electronic characters of the individual Rydberg levels necessary for this comparison are provided in Table II. It is known that the NO $I\ ^2\Sigma^+$ and $A'^2\Sigma^+$ states possess nearly pure *gerade* and *ungerade* characters, respectively.[47] Because all the f Rydberg levels investigated in our experiment possess the $f\sigma$ character that interacts with both the I and A' states, the electronic coupling mechanism can explain the production of both even-l and odd-l partial waves from vibrational autoionization of the f Rydberg levels. As shown in Table II, the s Rydberg levels investigated in our experiment are mostly combinations of the $s\sigma$, $d\sigma$, and $d\delta$ Rydberg characters. Because the $s\sigma$, $d\sigma$-$I\ ^2\Sigma^+$ coupling discussed above is expected to produce mostly even-l partial waves in the ionization continuum, the odd-l partial waves generated in vibrational autoionization of the s Rydberg levels should be accounted for by the vibrational coupling mechanism or by the $d\delta$-$B'^2\Delta$ coupling.

The behavior of the p Rydberg levels provides an interesting contrast to those of the s and f Rydberg levels. Table II shows that the $13p$ ($v=1$, $N=19$, $N_R^+=19$) level has pure $p\pi$ character. Despite the strong $p\pi$-$B,L\ ^2\Pi$ coupling mentioned above our analysis shows that the ionization continuum is dominated by p partial waves when the $13p$ ($v=1$, $N=19$, $N_R^+=19$) level autoionizes. In addition, the near absence of $N^+=17$ and $N^+=21$ photoelectron peaks in Fig. 2(a) are consistent with the generation of $p\pi$ rather than $p\sigma$ waves,[16] which validates the assumption in the previous MQDT calculations.[41,42] This behavior is not restricted to the $13p$ ($v=1$, $N=19$, $N_R^+=19$) level and is generally observed for the np ($v=1$, $N=19$, $N_R^+=19$) levels with $n=11$–15.[25] Being valence states, the $B\ ^2\Pi$ and $L\ ^2\Pi$ states are expected to carry more than $p\pi$ partial-wave character, and hence the sole production of $p\pi$ partial waves from vibrational autoionization of the np ($v=1$, $N=N_R^+$) levels is rather puzzling if the electronic coupling is the primary mechanism for these autoionization events. The vibrational autoionization events of the np ($v=1$, $N=18$ and 20, $N_R^+=19$) levels are, on the other hand, accompanied by more significant generation of even-l partial waves.[25] These Rydberg levels possess both $p\pi$ and $p\sigma$ character and interact not only with the $B\ ^2\Pi$ and $L\ ^2\Pi$ states but also with the $A'^2\Sigma^+$ state. Because the $A'^2\Sigma^+$ state is almost purely *ungerade* in character and hence cannot explain the production of even-l waves, the generation of even-l waves from vibrational autoionization of the np ($v=1$, $N=18$ and 20, $N_R^+=19$) levels indicates that

the vibrational coupling mechanism plays a role in these autoionization events.

IV. CONCLUSION

We have presented rotationally resolved photoelectron spectra from vibrational autoionization of individual rotational levels of the nl_R ($v=1$, $11 \leqslant n \leqslant 15$, $0 \leqslant l_R \leqslant 3$) Rydberg states of NO. With the possible exception of the photoelectron spectrum from the $13p$ ($v=1$, $N=19$, $N_R^+=19$) Rydberg level, all the spectra reported here show evidence for production of both even-l and odd-l partial waves from vibrational autoionization of a given nl_R Rydberg levels of NO, and thus demonstrate angular momentum exchange between the outgoing electron and the molecular-ion core induced by the vibrational quantum change of the core. The observed ion rotational state distributions are found to be strongly dependent on various quantum numbers associated with the autoionizing Rydberg state. Our experimental finding clearly illustrates that the interaction between the Rydberg electron and the vibrating dipolar core is important in the autoionization events of NO Rydberg levels, contrary to common assumptions in previous MQDT calculations. The angular momentum exchange observed in our experiment can be explained either by the vibrational coupling mechanism or the electronic coupling mechanism proposed earlier,[66] although we cannot determine the relative importance of the two mechanisms based solely on our experimental data.

ACKNOWLEDGMENTS

We thank R. J. Green and I. M. Konen for helpful discussions. This work was supported by the National Science Foundation under Grant No. PHY-9320356.

[1] R. S. Mulliken, J. Am. Chem. Soc. **86**, 3183 (1964).
[2] H. Lefebvre-Brion and R. W. Field, *Perturbations in the Spectra of Diatomic Molecules* (Academic, New York, 1986).
[3] C. H. Greene and Ch. Jungen, Adv. At. Mol. Phys. **21**, 51 (1985).
[4] H. Nakamura, Int. Rev. Phys. Chem. **10**, 123 (1991).
[5] G. Herzberg and Ch. Jungen, J. Mol. Spectrosc. **41**, 425 (1972).
[6] M. Schwarz, R. Duchowicz, W. Demtröder, and Ch. Jungen, J. Chem. Phys. **89**, 5460 (1988).
[7] C. Bordas, P. Labastie, J. Chevaleyre, and M. Broyer, Chem. Phys. **129**, 21 (1989).
[8] Ch. Jungen, S. T. Pratt, and S. C. Ross, J. Phys. Chem. **99**, 1700 (1996).
[9] W. G. Wilson, K. S. Viswanathan, E. Sekreta, and J. P. Reilly, J. Phys. Chem. **88**, 672 (1984).
[10] S. W. Allendorf, D. J. Leahy, D. C. Jacobs, and R. N. Zare, J. Chem. Phys. **91**, 2216 (1989).
[11] D. J. Leahy, K. L. Reid, and R. N. Zare, J. Chem. Phys. **95**, 1757 (1991).
[12] D. J. Leahy, K. L. Reid, H. Park, and R. N. Zare, J. Chem. Phys. **97**, 4948 (1992).
[13] M.-T. Lee, K. Wang, V. McKoy, R. G. Tonkyn, R. T. Wiedmann, E. R. Grant, and M. G. White, J. Chem. Phys. **96**, 7848 (1992).
[14] H. Park and R. N. Zare, J. Chem. Phys. **99**, 6537 (1993).
[15] H. Park and R. N. Zare, Chem. Phys. Lett. **225**, 327 (1994).
[16] H. Park and R. N. Zare, J. Chem. Phys. **104**, 4554 (1996).
[17] H. Park and R. N. Zare, J. Chem. Phys. **104**, 4568 (1996).
[18] Y. Achiba and K. Kimura, Chem. Phys. **129**, 11 (1985).
[19] J. Kimman, J. W. J. Verschuur, M. Lavollee, H. B. van Linden van den Heuvell, and M. J. van der Wiel, J. Phys. B **19**, 3909 (1986).
[20] S. T. Pratt, P. M. Dehmer, and J. L. Dehmer, J. Chem. Phys. **85**, 5535 (1986).
[21] J. L. Dehmer, P. M. Dehmer, J. B. West, M. A. Hayes, M. R. S. Siggel, and A. C. Parr, J. Chem. Phys. **97**, 7911 (1992).
[22] J. Guo, A. Mank, and J. W. Hepburn, Phys. Rev. Lett. **74**, 3584 (1995).
[23] J. L. Dehmer, P. M. Dehmer, S. T. Pratt, F. S. Tomkins, and M. A. O'Halloran, J. Chem. Phys. **90**, 6243 (1989).
[24] S. T. Pratt, E. F. McCormack, J. L. Dehmer, and P. M. Dehmer, J. Chem. Phys. **92**, 1831 (1990).
[25] H. Park, D. J. Leahy, and R. N. Zare, Phys. Rev. Lett. **76**, 1591 (1996).
[26] E. Miescher and K. P. Huber, in *International Review of Science* (Butterworths, London, 1976), Vol. 2, p. 37.
[27] E. Miescher, Can. J. Phys. **54**, 2074 (1976).
[28] W. Y. Cheung, W. A. Chupka, S. D. Colson, D. Gauyacq, P. Avouris, and J. J. Wynne, J. Chem. Phys. **78**, 3625 (1983).
[29] Y. Anezaki, T. Ebata, N. Mikami, and M. Ito, Chem. Phys. **89**, 103 (1984).
[30] Y. Anezaki, T. Ebata, N. Mikami, and M. Ito, Chem. Phys. **97**, 153 (1985).
[31] Y. Achiba, K. Sato, and K. Kimura, J. Chem. Phys. **82**, 3959 (1985).
[32] J. W. J. Verschuur, J. Kimman, H. B. van Linden van den Heuvell, and M. J. van der Wiel, Chem. Phys. **103**, 359 (1986).
[33] S. Fredin, D. Gauyacq, M. Horani, Ch. Jungen, G. Lefevre, and F. Masnou-Seeuws, Mol. Phys. **60**, 825 (1987).
[34] D. T. Biernacki, S. D. Colson, and E. E. Eyler, J. Chem. Phys. **88**, 2099 (1988).
[35] D. T. Biernacki, S. D. Colson, and E. E. Eyler, J. Chem. Phys. **89**, 2599 (1988).
[36] G. E. Gadd, L. E. Jusinski, and T. G. Slanger, J. Chem. Phys. **91**, 3378 (1989).
[37] S. T. Pratt, Ch. Jungen, and E. Miescher, J. Chem. Phys. **90**, 5971 (1989).
[38] A. Nussenzweig and E. E. Eyler, J. Chem. Phys. **101**, 4617 (1994).
[39] A. Fujii and N. Morita, Chem. Phys. Lett. **182**, 304 (1991).
[40] A. Fujii and N. Morita, J. Chem. Phys. **97**, 327 (1992).
[41] A. Giusti-Suzor and Ch. Jungen, J. Chem. Phys. **80**, 986 (1984).
[42] M. Raoult, J. Chem. Phys. **87**, 4736 (1987).
[43] K. Nakashima, H. Nakamura, Y. Achiba, and K. Kimura, J. Chem. Phys. **91**, 1603 (1989).
[44] Ch. Jungen, J. Chem. Phys. **53**, 4168 (1970).
[45] R. Gallusser and K. Dressler, J. Chem. Phys. **76**, 4311 (1982).
[46] R. de Vivie and S. D. Peyerimhoff, J. Chem. Phys. **89**, 3028 (1988).
[47] H. Sun and H. Nakamura, J. Chem. Phys. **93**, 6491 (1990).
[48] H. Park, Ph.D. thesis, Stanford University, 1995.
[49] U. Fano and J. W. Cooper, Rev. Mod. Phys. **40**, 441 (1968).
[50] E. E. Nikitin and R. N. Zare, Mol. Phys. **82**, 85 (1994).
[51] In literature, the quantum number $\mathscr{L}$ that denotes the projection of the electronic orbital angular momentum $\vec{l}_R$ on the rotational axis of the core is often used to designate the Rydberg level in Hund's case (d) limit. Because $\mathscr{L} = N - N_R^+$, $\mathscr{L}$ becomes redundant once N and N_R^+ are specified.
[52] G. Herzberg, *Molecular Spectra and Molecular Structure I. Spectra of Diatomic Molecules*, 2nd ed. (Van Nostrand, Toronto, 1950).
[53] K. P. Huber and G. Herzberg, *Molecular Spectra and Molecular Structure. IV. Constants of Diatomic Molecules* (Van Nostrand Reinhold Company, New York, 1979).
[54] E. Miescher and F. Alberti, J. Phys. Chem. Ref. Data **5**, 309 (1976).
[55] E. S. Chang and U. Fano, Phys. Rev. A **6**, 173 (1972).
[56] G. P. Bryant, Y. Jiang, M. Martin, and E. R. Grant, J. Chem. Phys. **101**, 7199 (1994).
[57] I. Kovacs, *Rotational Structure in the Spectra of Diatomic Molecules* (Elsevier, New York, 1969).
[58] S. N. Dixit and V. McKoy, Chem. Phys. Lett. **128**, 49 (1986).
[59] J. Xie and R. N. Zare, J. Chem. Phys. **93**, 3033 (1990).
[60] R. N. Zare, *Angular Momentum* (Wiley–Interscience, New York, 1988).
[61] H. Park, I. M. Konen, and R. N. Zare (unpublished).
[62] S. Ross and Ch. Jungen, Phys. Rev. Lett. **59**, 1297 (1987).
[63] A. L. Roche and Ch. Jungen, J. Chem. Phys. **98**, 3637 (1993).
[64] R. S. Berry and S. E. Nielsen, Phys. Rev. A **1**, 395 (1970).
[65] E. Rabani and R. D. Levine, J. Chem. Phys. **104**, 1937 (1996).
[66] A. Giusti-Suzor and H. Lefebvre-Brion, Chem. Phys. Lett. **76**, 132 (1980).
[67] R. S. Berry, J. Chem. Phys. **45**, 1228 (1966).
[68] E. E. Eyler, Phys. Rev. A **34**, 2881 (1986).